APPENDIX B

THE MECHANICAL POLISHING PROCESS BASED ON PIN-ON-DISK EXPERIMENTS

In many works on the material removal in the Chemical Mechanical Process (CMP), the effects of several process parameters have been addressed. However, a thorough understanding of the mechanisms of material removal and a model to correlate the process parameters to material removal rate (MRR) are still lacking. This appendix develops such models for polishing based on the results from the pin-on-disk experiments with emphasis on the mechanical aspects of CMP. The pin-on-disk apparatus offers a quick way to conduct polishing experiments and thus identify the significance of such process parameters as the abrasion mode, abrasive size, abrasive concentration, and hardness of material abraded on MRR and Preston constant. Process optimization schemes for enhancing MRR and Preston constant are also proposed.

B.1 Introduction

Chemical Mechanical Polishing (CMP) has become a primary method for planarization of semiconductor wafers. The present CMP process is a tribo-chemical process. The material coated on the wafer surface, such as silicon dioxide, silicon nitride and metals (commonly aluminum, copper, their alloys and tungsten (Hetherington, 1996), reacts with the chemicals in the slurry to form a softer surface layer. Subsequently, this layer is removed by mechanical abrasion of the slurry particles against the wafer surface (Liang et al., 1997). Since the present CMP involves chemicals to assist the mechanical wear, the slurry composition should be changed and the pad should be cleaned or replaced when sequentially polishing different materials on the wafer surface. It is time consuming and not cost-effective. In addition, the use of chemicals increases the complexity of the process and its control. Therefore may increase the variation of process outputs (such as thickness, uniformity of the coating) and the difficulty of machine design. The ideal way is to design a mechanical-dominated process to improve the controllability and quality of the "CMP". To achieve this objective, the mechanism regarding the abrasive wear in the typical CMP conditions (pressure, velocity, materials, etc.) should be studied.

In this appendix, two proposed processes, two-body and three-body wear, for either planarization or polishing are examined in terms of the friction coefficient, Preston coefficient, and wear coefficient with respect to the grit size effect. The experimental results are compared with the capability of the present CMP process and discussed. Moreover, the results of this study will be used for the test machine design for a real research project for testing a real wafer with the same coating materials in the near future.

The abrasive wear has been studied for decades. Recently, several critical experiments were performed to understand and model the friction and wear mechanisms under abrasive sliding situations by Sin, Saka, and Suh (1979). The size of the abrasive particles ranges from 10 μm to 250 μm, and the materials studied are polymethyl methacrylate, pure nickel, AISI 1095 steel, and OFHC copper. The results can be summarized as follows:

(1) The friction coefficient, wear rate, and wear coefficient increase with the grit size up to a critical size.

(2) The friction coefficient does not vary much with materials, and for metals it does not depend much on the applied load.

(3) The number of contacting particles increases approximately linearly with the applied load and varies inversely as the square of the grit diameter.

(4) Plowing is dominant during abrasion. The groove width increases linearly with the grit diameter. The load has little influence on the groove width.

This research is based on the same experimental methodology. However, the size of the particles will cover smaller grit sizes (0.05 μm to 3 μm) and the worn materials are pure metals: aluminum, copper and tungsten.

B.2 Experimental

B.2.1 Apparatus. Figure B.1 shows the pin-on-disk apparatus. The pin is cylindrical and flat-ended with a diameter of about 6.35 mm (0.25 in) and held by the specimen holder. The edge of the pin is chamfered to increase the contact area when the pin was not mounted perpendicularly to the pad surface. The normal load is provided by a dead weight added on the top of the specimen holder. The friction force is measured by the strain gage bridge on the strain ring corresponding to a voltage change at the output of the strain gage set. The output voltage of the strain gage bridge is recorded by a chart recorder. The aluminum disk is driven by a DC gear motor with a speed controller to control the angular speed. In two-body wear tests, alumina abrasive papers are attached the disk. In three-body wear tests, a lapping pad is used and the slurry is confined on the surface of the pad by clamping a plastic strip around the circumference of the disk.

B.2.2 Experimental Conditions and Test Materials. In two-body wear tests, aluminum abrasive papers with grit size 3000, 1000, 300, and 50 nm were used in dry sliding conditions shown on Table B.1. Figure B.2 shows the micrographs of the surfaces of the abrasive papers with grit size 3000, 1000, and 300 nm, respectively. It can be seen that the size distribution is large. And the shapes and orientations of the abrasive particles are irregular. The normal load was varied between 1.47 N (0.15 kg) and 3.92 N (0.4 kg) to obtain substantial weight loss throughout all the experiments. The angular velocity of the disk was held constant at 63.2 rpm. The diameter of the sliding track was adjusted for each experiment to ensure that the specimen always passes over the fresh abrasive and so that the sliding velocity was varied from 0.22 m/s to 0.65 m/s along the track. The specimens were weighed to an accuracy of 0.01 mg before testing. After testing, the specimens were rinsed by distilled water and the weight is measured again after drying.

In the three-body wear test, a commercial synthetic polishing pad for metallographic specimen polishing, especially suitable for micro-polishing of integrated circuit (IC) devices, was used. Water-based, deagglomerated slurries with abrasive particle sizes 1000 nm (α alumina), 300 nm (α alumina), and 50 nm (15% of α and 85% of γ alumina) were poured on the polishing pad. In order to maintain the fresh abrasive, the slurry with worn abrasive

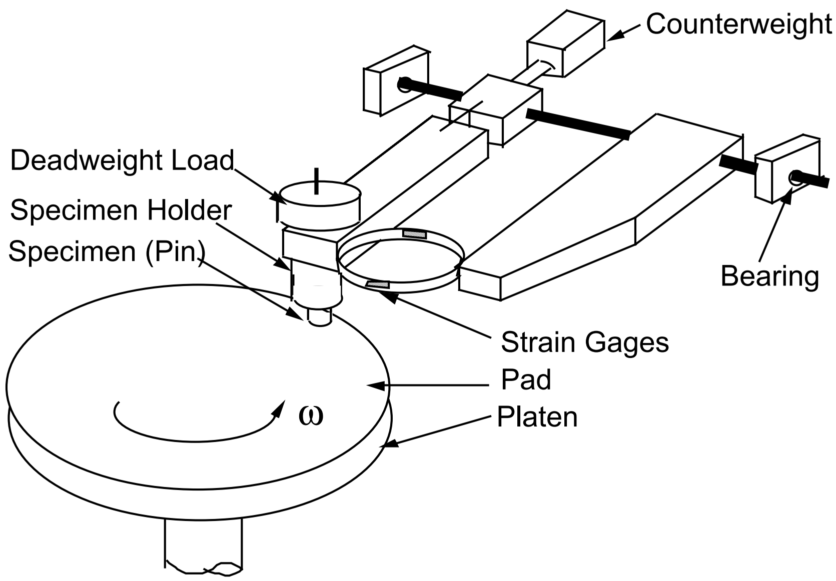

Figure B.1 Schematic of the pin-on-disk apparatus.

Table B.1: Experimental conditions.

Experimental Parameters	Abrasion Modes Two-body	Three-body	CMP (typical)
Normal Load (N)	1.5 - 4.0	1.5 - 4.0	1,343
Nominal Pressure (MPa)	0.05 - 0.13	0.05 - 0.13	0.04
(psi)	(6.7 - 17.8)	(6.7 - 17.8)	(6)
Angular Speed of the platen (rpm)	60	60	25
Sliding Velocity (m/s)	0.5	0.5	0.5
Sliding Duration (min)	2 - 4	2 - 4	2 – 4
Sliding Distance (m)	60 – 120	60 - 120	60 – 120
Abrasive Material	Al_2O_3	Al_2O_3	Al_2O_3
Abrasive Diameter (nm)	50,300 1000,3000	50, 300, 1000	200

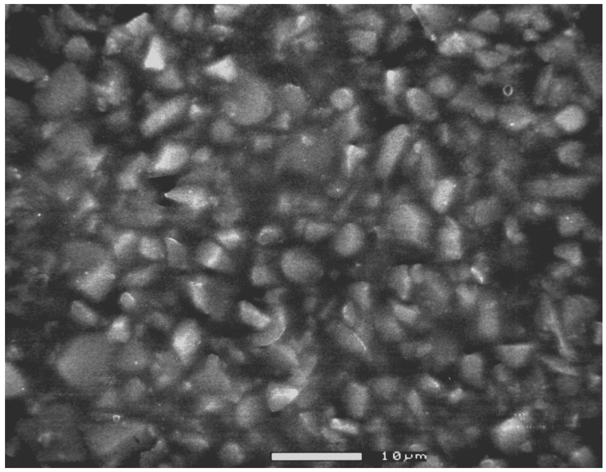

(a)

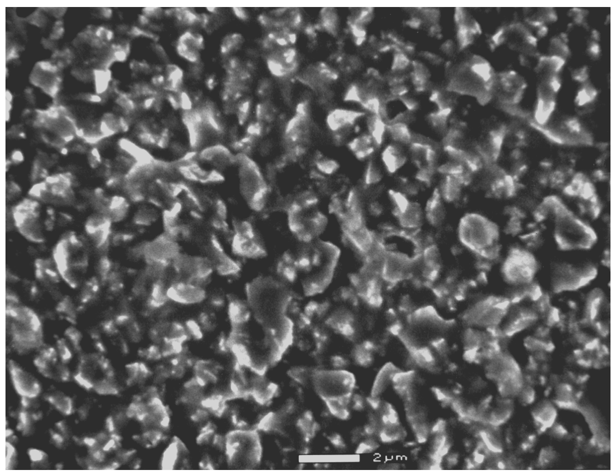

(b)

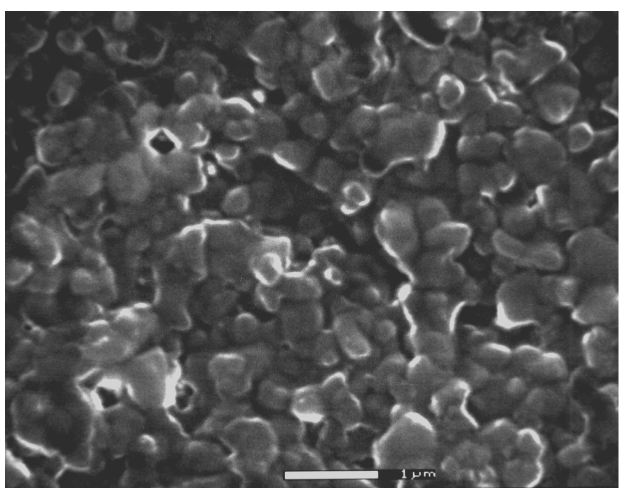

(c)

Figure B.2 Micrographs of the abrasive surfaces of lapping films with grit sizes (a) 3,000 nm (b) 1,000 nm, and (c) 300nm.

particles and wear particles was removed after few runs. The sliding track was also varied to prevent abrading the same area on the pad. Table B.1 also gives the load, angular velocity, sliding distance and other experimental conditions for the three-body wear tests, which are essentially similar to the prior two-body dry sliding tests. The weight loss was also measured by following the same procedures. Three different pure metals, Al (99%) and Cu (99.98%) and W (99.9%), which are usually coated on the wafer surface for wiring and conductive plug, were employed in the wear tests. Some of the important physical and mechanical properties of these three metals are listed in Table B.2. The specimens were cut by a band saw from the rods and machined on a lathe for coarse surface finish and ensured the worn surface was parallel to the sliding distance. Then the specimens were polished by a metallographic polisher with the abrasive grit size down to 0.05 μm (equal to the smallest size used in the wear tests) to ensure the surface characteristics produced by experiments can be identified. Then the specimens were cleaned and dried.

B.3 Results

B.3.1 Two-body Wear. The friction coefficients of Al, Cu and W versus the abrasive grit size of alumina is shown in Fig. B.3. For all three materials, the friction coefficient increases with the abrasive grit size except the grit size of 50 nm. For examples, the mean friction coefficient increases from 0.5 to 0.65 approximately as the grit size increases from 300 nm to 3000 nm. The mean values of friction coefficients of the three materials corresponding to different grit sizes are listed in Table B.3. At the grit size of 50 nm, surprisingly high friction coefficients was recorded. Figure B.4 shows such a plot of the friction coefficient of Cu versus the sliding distance. In this figure, the friction coefficient sometimes suddenly increases and then followed by a drop. The possible explanation for such a high value of friction coefficient and a sudden change on friction coefficient are attributed to the wear particles agglomerate at the sliding interface and consequently break off (Oktay and Suh, 1992). Indeed, deep large plowing grooves were found on the 50 nm abrasive paper. This may support the existence of agglomeration at the interface and thus cause the high stress on the tip of the agglomerates to severely plow the surface of the abrasive paper due to the load is supported by a few agglomerates.

Table B.2: Experimental materials.

Material	Purity (%)	Density (kg/m^3)	Young's Modulus (GPa)	Hardness (MPa)
Al	99.00	2,699	62	392
Cu	99.98	8,940	112	784
W	99.90	19,300	408	3,430

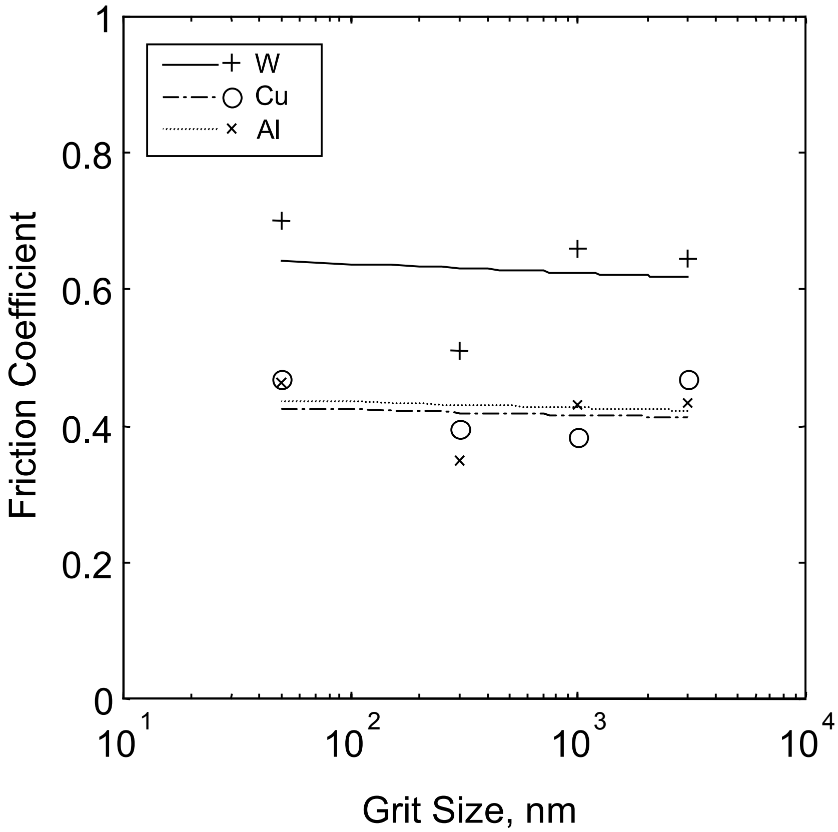

Figure B.3 Friction coefficient versus the nominal diameter of the abrasive particles in two-body wear conditions.

Table B.3: Experimental results for two-body wear conditions.

Material	Abrasive Diameter (nm)	Friction Coefficient	Wear Rate (m^3/m)	Preston Constant (MPa^{-1})	Wear Coefficient
Al	3,000	0.44	$0.315\ x10^{-10}$	$0.210x10^{-4}$	0.0084
	1,000	0.43	$1.077x10^{-10}$	$0.718x10^{-4}$	0.0287
	300	0.34	$0.838x10^{-10}$	$0.210x10^{-4}$	0.0084
	50	0.46	$0.297x10^{-10}$	$0.074x10^{-4}$	0.0030
Cu	3,000	0.47	$2.144x10^{-10}$	$1.430x10^{-4}$	0.1144
	1,000	0.39	$1.023x10^{-10}$	$0.820x10^{-4}$	0.0656
	300	0.39	$0.809x10^{-10}$	$0.203x10^{-4}$	0.0162
	50	0.48	$0.466x10^{-10}$	$0.116x10^{-4}$	0.0093
W	3,000	0.65	$0.518x10^{-10}$	$0.345x10^{-4}$	0.1208
	1,000	0.66	$0.138x10^{-10}$	$0.092x10^{-4}$	0.0321
	300	0.51	$0.286x10^{-10}$	$0.071x10^{-4}$	0.0250
	50	0.70	$0.124x10^{-10}$	$0.031x10^{-4}$	0.0108

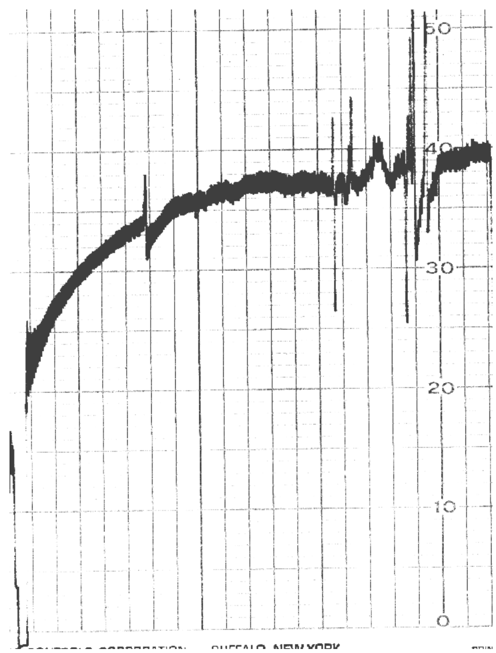

Figure B.4 Friction force measurement (y-axis: 10 unit = 20 gf, normal load is 200 gf) on Cu versus sliding distance (x-axis).

In order to study the effect of grit size on the wear of specimen, the volume wear rate, the Preston constant and the wear coefficient are examined versus the abrasive grit size. The definitions of the volume wear rate *R*, Preston constant k_p, and wear coefficient k_w are as following:

$$R = \frac{V}{S} \tag{B.1}$$

$$k_p = \frac{V}{SL} \tag{B.2}$$

$$k_w = \frac{VH}{SL} \tag{B.3}$$

In the polishing of semiconductor devices, the rate of the thickness change is more important than the rate of the volume removal since the globally uniform removal of material across the wafer is more important than the amount of material removed. It has been empirically found that the thickness reduction rate is proportional to the nominal pressure, based on the apparent contact area, and the linear velocity of the worn surface of the specimens. Thus the Preston constant can be defined as the ratio of the thickness reduction rate $d\xi/dt$ divided by the nominal pressure p and the relative velocity v_R. This definition of Preston constant is identical with that in Eq. (B.2). We can divide both the numerator and denominator of the left-hand side of Eq. (B.2) by the nominal area of contact, and then rearrange it and differentiate by time t. This leads to:

$$\frac{d\xi}{dt} = k_p p v_R \tag{B.4}$$

where the thickness reduced ξ and nominal pressure p equal to the volume worn V and the load L divided by the nominal contact area A, respectively. Equation 4 can be used to evaluate the polishing rate only when the thickness reduced is in the global range instead of on the scale of polishing of local surface roughness so that the use of the nominal pressure is meaningful.

Figures B.5 and B.6 show the Preston constant and the wear coefficient of Al, Cu and W versus the grit size, respectively. And Table B.3 also list all the mean values of wear rate, Preston constant, and wear coefficient for two-body wear. Those values increase with the grit size between the size ranging from 50 nm to 300 nm. The wear rate of Cu and W increase by a factor of three and the Preston constant of these two materials increase by an order of magnitude when the grit size increases from 50 nm to 300 nm. Compared with Cu and W, the wear rate and Preston constant of Al does not significantly change when the grit size increases. For Cu and W, the experimental results show the wear coefficients are on the same range and increase with the grit size similarly (the wear coefficient increases about an order of magnitude when grit size increases from 50 nm to 300 nm); while the wear coefficient of Al is less than those of Cu and W (approximately a factor of 5 smaller) and increase slower than the those of the other two materials. It is suspected that the decrease of the wear rate, Preston constant and wear coefficient of Al is attributed to the clogging and capping of the abrasive materials by the soft wear particles so that the effective wear particles are much less than those of the other two cases. On the other hand, an aluminum oxide layer (alumina) may easily form on the contact surface due to the elevated flash temperature by dry sliding at the fast enough velocity. This may have some effect on the wear rate due to oxidation-dominated wear is generally slower than the wear due to the plasticity-dominated wear at the same loading condition (Lim and Ashby, 1987) . Indeed, on both the sliding tracks and the surface of the Al specimen, thin dark-color layers of material different from the abrasive and pure aluminum were found, which are suspected to be oxide layers and wear particles.

B.3.2 Three-body Wear. The experimental results of friction coefficient versus the grit size in the three-body wear are shown in Figure B.7. The friction coefficient increases with the grit size for all three materials. Table 4 lists the mean values of measured friction coefficient with different grit size. All these values suggest that the interfacial conditions did not reach boundary lubrication regime. The asperities of the specimens directly contact with the pad surface and thus contribute to the genesis of friction. Compared with the two-body wear, the friction coefficient of Al and Cu is slightly higher for all three grit size used (the friction coefficient increase 1.5 and copper 0.05, approximately). However, the friction coefficient of W decreases by about 0.2.

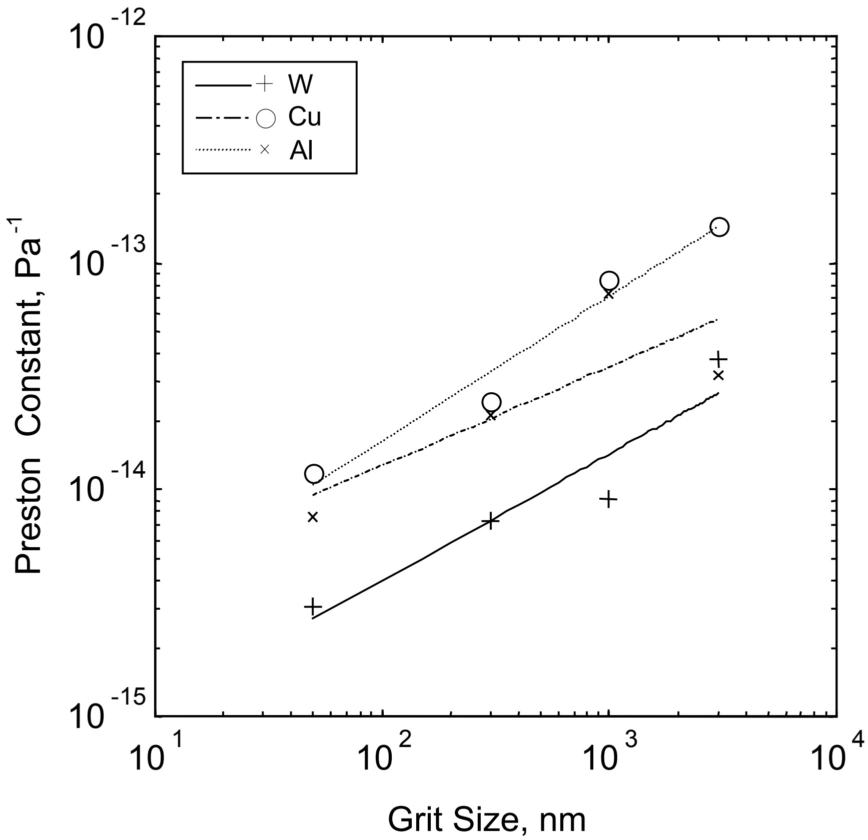

Figure B.5 Preston constant versus the nominal diameter of the abrasive particles in two-body wear conditions.

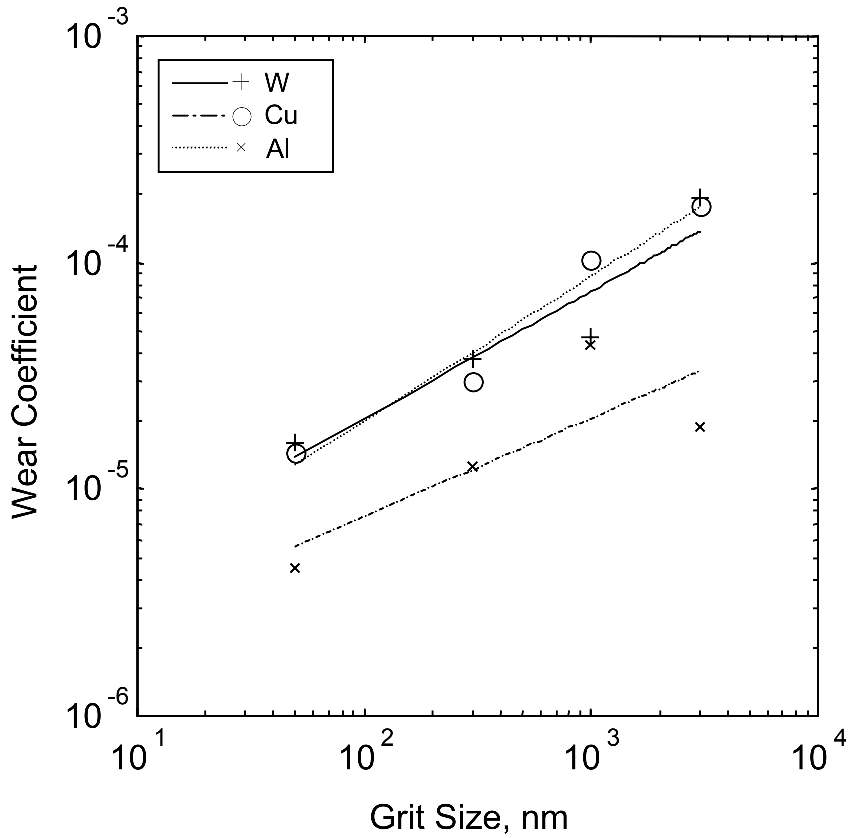

Figure B.6 Wear coefficient versus the nominal diameter of the abrasive particles in two-body wear conditions.

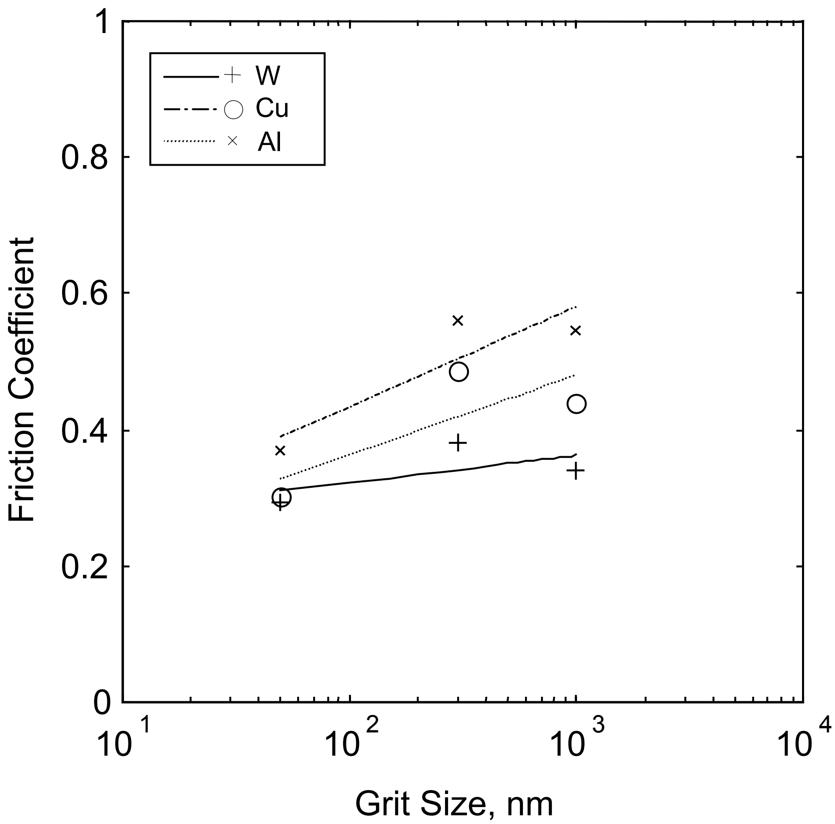

Figure B.7 Friction coefficient versus the nominal diameter of the abrasive particles in three-body wear conditions.

Table B.4: Experiment results for three-body wear conditions.

Material	Abrasive Diameter (nm)	Friction Coefficient	Wear Rate (m^3/m)	Preston Constant (MPa^{-1})	Wear Coefficient
Al	1,000	0.55	4.533×10^{-10}	3.022×10^{-4}	0.1209
	300	0.56	4.034×10^{-10}	2.690×10^{-4}	0.1076
	50	0.37	1.488×10^{-10}	0.498×10^{-4}	0.0199
Cu	1,000	0.44	3.894×10^{-10}	2.596×10^{-4}	0.2077
	300	0.48	4.395×10^{-10}	2.930×10^{-4}	0.2344
	50	0.30	0.758×10^{-10}	0.253×10^{-4}	0.0202
W	1,000	0.34	0.199×10^{-10}	0.133×10^{-4}	0.0464
	300	0.38	0.225×10^{-10}	0.152×10^{-4}	0.0531
	50	0.29	0.098×10^{-10}	0.034×10^{-4}	0.0120

Figures B.8 and B.9 show the dependence of Preston constant and wear coefficient on the abrasive grit size. The Preston constant and wear coefficient all increase with the grit size. Although it seems that those values increase at much slower rates with the grit size up to 300 nm, it is hard to say that there exist a critical grit size just based on the three average data points. More different grit sizes should be tested to find out the trend of the effect of grit size on the wear and thus to understand the mechanism(s) behind. It is also been found that the Preston constant and wear coefficient of three-abrasion wear at the same grit size are higher than those of prior two-body wear cases. The wear mechanism is determined by the interaction of the specimen material, the abrasive particles, the lubricant (slurry) and the pad. The Preston constant and wear coefficient thus are determined by the parameters affect those four components (the specimen, abrasive, lubricant and pad). For example, the abrasive packing density and the orientation of the abrasive particles bonded on the papers will affect the rate of wear. It may tell nothing to just compare the wear rate between the two-body and three-body wear without knowing the interfacial characteristics for both cases. On the other hand, the small particles in the slurry may agglomerate into larger size particles and affect the wear rate. However, the plotting of Figs. B.8 and B.9 does not account for this effect. This is one of the possible reasons which causes the wear rate, Preston constant and wear coefficient are larger in three-body wear tests. More characterization on the abrasive surface of the lapping paper and agglomeration in the slurry should be done in the future to understand the polishing process and develop the approach to increase the wear of materials.

B.3.3 The Effect of Hardness on the Preston Constant. Figures B.10 and B.11 show that the Preston constant decreases with the increase of the hardness of the materials in both the two-body and three-body wear with grit size ranging from 50 nm to 300 nm. A similar correlation has been found by using a larger grit size to test numbers of single-phase materials (Suh, 1986). In Figs. B.10 and B.11, it is also found that the Preston constant ratio of Cu to W is approximately the same, regardless of the grit size. The factor is about 4 for the two-body wear tests and 15 for the three-body wear tests. In addition, in Fig. B.11, there seems a critical grit size (between 300 nm to 1000 nm) above which the Preston constant will increase much more slowly with increase of the grit size.

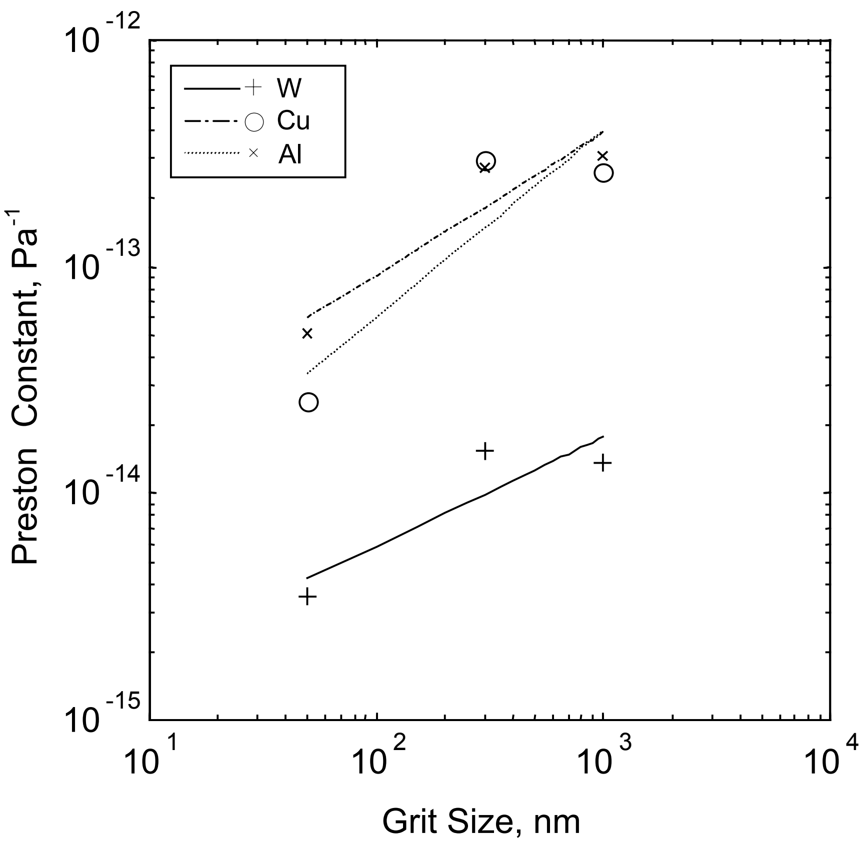

Figure B.8 Preston constant versus the nominal diameter of the abrasive particles in three-body wear conditions.

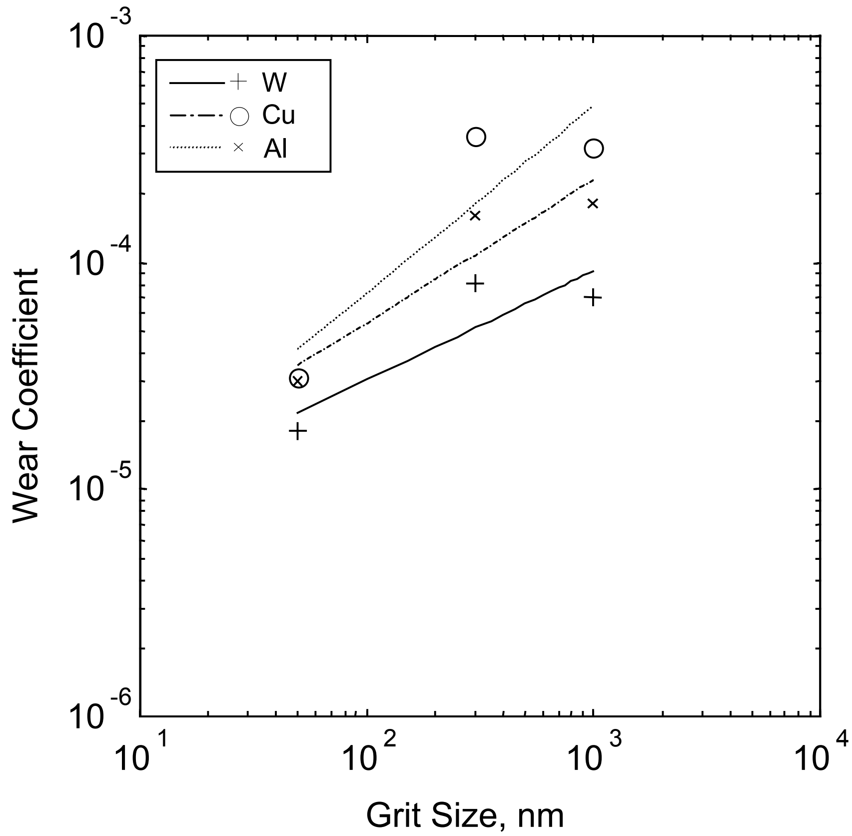

Figure B.9 Wear coefficient versus the nominal diameter of the abrasive particles in three-body wear conditions.

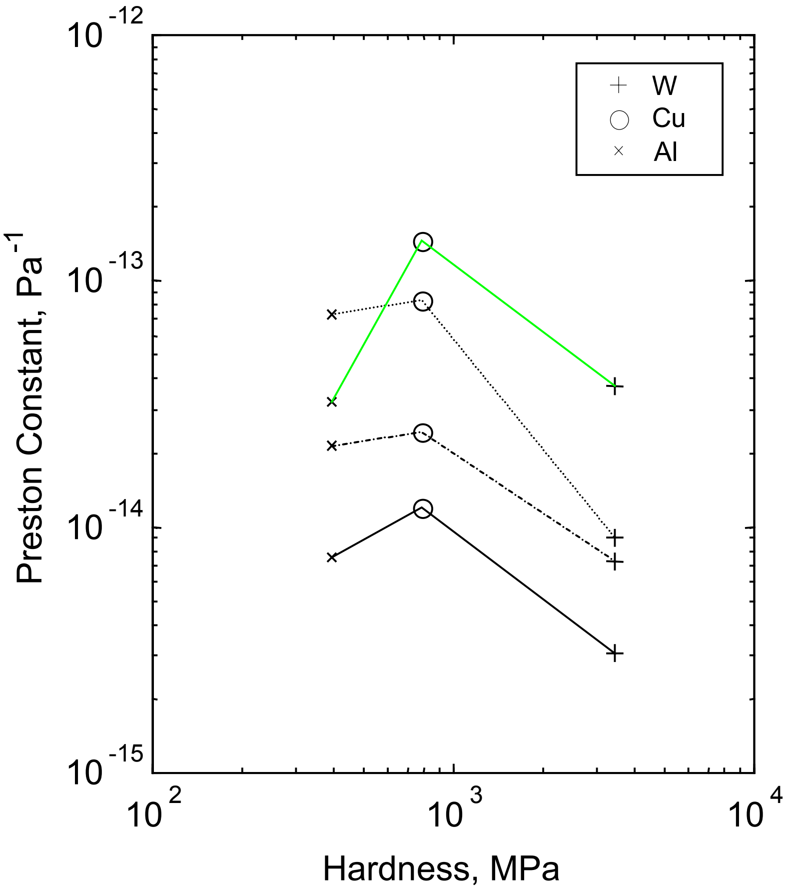

Figure B.10   Preston constant versus the hardness of the slid material in two-body wear conditions.

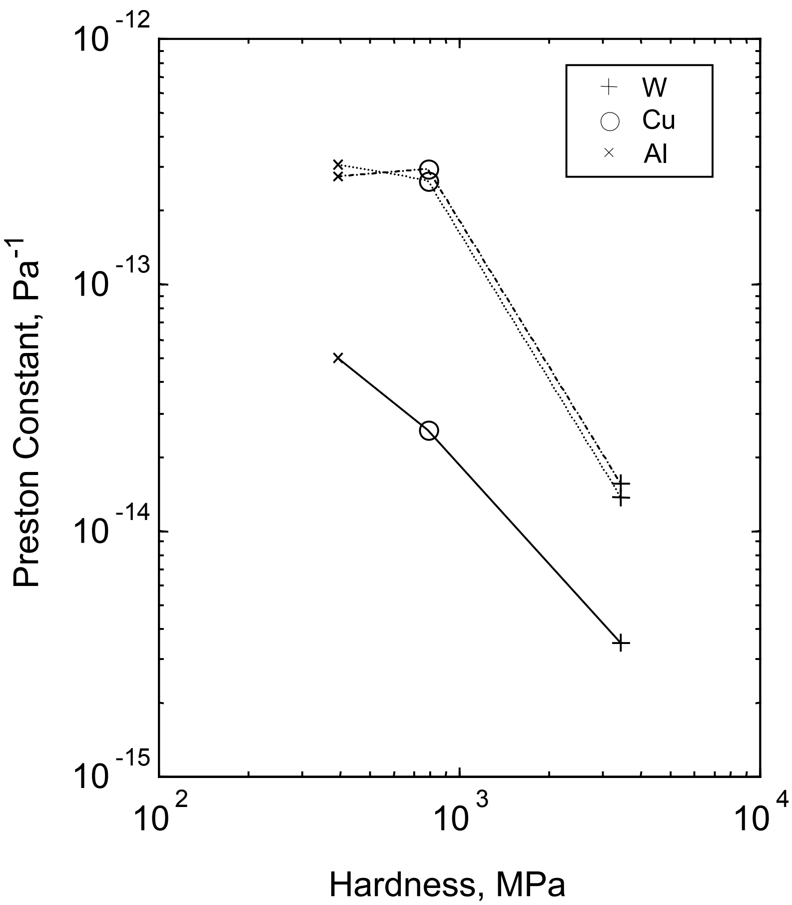

Figure B.11 Preston constant versus the hardness of the slid material in three-body wear conditions.

B.4 Discussion

It might be difficult to predict the wear behaviors on a 100 mm dia. or larger-size wafer by a simple interpretation of the results from this pin-on-disk set-up because the kinematics of the wafer-pad system and the interfacial conditions might be different. However, it is possible to get the same range of friction coefficient and the very rough order-of-magnitude estimation about the Preston constant, and wear coefficient by these experiments since the specimen diameter is much larger than the particle size used. On the basis of this assumption, the Preston constant of the present CMP is compared with the experimental results. The Preston constants of the present CMP process are calculated by using the typical process conditions presented in the literature, which is also listed in Table B.1 (Muraka et al., 1993; Heterington et al., 1996). The size of abrasive particles in the CMP process is the nominal median agglomerate size of 200 nm, and the size chosen for comparison in both two-body and three-body wear modes is 200 nm. The comparison is listed in Table B.5.

It shows that the Preston constant for the current CMP process is about two orders of magnitude less than the experimental results for both copper and tungsten polishing. It should be noted that the worn volume in the CMP case is calculated by multiplying the height removed with the nominal area of the wafer. This might not be quite true for a patterned wafer. The ratio of the nominal area of the wafer to the projected area of the high features ranges from 100 to 1 (1 for blanket wafers). Thus Preston constant of the CMP process might be comparative to those from the experiments. Besides, as mentioned earlier the particles size in the three-body wear conditions might be larger due to agglomeration. This may also attribute to the larger Preston constant estimated by the experiments. On the other hand, the Preston constants of Cu and W in the CMP are close. Nevertheless, either for the two- or three-body wear conditions, the Preston constant of copper is about an order of magnitude larger than that of the W. This is due to the assistance of the chemistry in the CMP greatly increases the Preston constant by converting the metal surface to a more readily abraded material (oxide).

Table B.5 Comparison of the Preston constant of Al, Cu, and W in two- and three- body wear experiments and the present CMP process. (The abrasive size is 200 nm.)

Material	Preston Constant (MPa^{-1})		
	Two-body Wear	Three-body Wear	Present CMP
Al	2.2×10^{-8}	1.3×10^{-7}	-
Cu	1.7×10^{-7}	1.0×10^{-7}	4.5×10^{-7}
W	5.9×10^{-9}	8.1×10^{-9}	5.9×10^{-7}

B.5 Conclusions

As a result of this study on the pin-on-disk type of polishing apparatus, the following conclusions can be drawn.

(1) The friction coefficient, wear rate, Preston constant and wear coefficient of the Al, Cu and W slid against the alumina lapping papers and polishing pads with alumina suspension slurries increase with the abrasive size.

(2) The Preston constant decreases with the increase of the hardness of these three materials by using the alumina abrasive particles.

(3) The Preston constant of Cu and W from the experimental results is about one to two orders of magnitude larger than those from the CMP process. However, the Preston constant varies only slightly for different materials (Cu and W) in the CMP process, but significantly in the experiments.

Based on this study, several routes are proposed to continue the research on the abrasive wear for the planarization and polishing of semiconductor coating materials:

(1) Characterize the surfaces of the lapping papers and polishing pad, and the size of the abrasive in the slurry.

(2) Collect more data form experiments to consolidate the conclusions above and extend the study of the mechanisms of both two-body wear and three-body wear in the CMP conditions.

(3) Study the effects of the grit size, load and other parameters on the topography of the worn surface.

(4) Use the slurry and pad in the state-of-the-art CMP process to compare with the estimation of the Preston constant based on the literature results.

(5) Use test wafers with the same conditions to study the effects of the grit size and other important parameters on the Preston constant and surface finish of the surface coating materials.

(6) Design new processes to robustly control the material removal and surface finish for wafer polishing on the basis of understanding the abrasive wear from this study and other literature.

Nomenclature

A_n = nominal contact area (m^2)
H = hardness of sliding surface (N/m^2)
k_w = wear coefficient
k_p = wear factor ($m^3/m\cdot N$)
L = load on the sliding surface (N)
p = nominal pressure (N/m^2)
R = volume wear rate (m^3/m)
S = sliding distance (m)
t = sliding time (s)
V = volume worn (m^3)
v_R = relative sliding velocity (m/s)
ξ = thickness of the material removed on wafer surface (m)

References

Hetherington, D.L., 1996, "Tungsten Chemical-Mechanical Polishing for ULSI Via Formation," *Surface Technology*, Rodel Inc.

Liang, H., Kaufman, F., Sevilla, R., and Anjur, S., 1997, "Wear Phenomena in Chemical Mechanical Polishing," *Wear*, Vol. 211, pp. 271-279.

Lim, S.C., and Ashby, M.F., 1987, "Wear-Mechanism Maps," *Acta Metall.*, Vol. 35, pp.1-24.

Murarka, S.P., Steigerwald, J., and Gutmann, R.J., 1993, "Inlaid Copper Multilevel Interconnections Using Planarization by Chemical-Mechanical Polishing," *MRS Bulletin*, June, 1993, pp. 46-51.

Oktay, S.T., and Suh, N.P., 1992, "Wear Debris Formation and Agglomeration," *ASME J. of Tribology*, Vol. 114, pp. 379-393.

Sin, H.-C., Saka, N., and Suh, N.P., 1979, "Abrasive Wear Mechanisms and the Grit Size Effect," *Wear*, Vol. 55, pp. 163-190.

Suh, N.P., 1986, *Tribophysics*, Prentice-Hall, Inc, p. 269.